

## Supporting information

### **Pulsed Electrochemical Deposition of Porous WO<sub>3</sub> on Silver Networks for Highly Flexible Electrochromic Devices**

Yanan Wang,<sup>a†</sup> Zhaohui Meng,<sup>a†</sup> Chen Hou,<sup>a</sup> Teng Li,<sup>a</sup> Dajiang Zheng,<sup>a</sup> Qingchi Xu,<sup>a</sup> Hao Wang,<sup>a</sup> Xiang Yang Liu<sup>\*ab</sup> and Wenxi Guo<sup>\*ac</sup>

<sup>a</sup>Research Institute for Biomimetics and Soft Matter, Fujian Provincial Key Laboratory for Soft Functional Materials Research, Department of Physics, Jiujiang Research Institute, Xiamen University, Xiamen 361005, China

<sup>b</sup>Department of Physics, Faculty of Science, National University of Singapore, Singapore, 117542, Singapore.

<sup>c</sup>Xiamen Univ, Shenzhen Research Institute, Shenzhen 518057, Peoples R China.

\*Email: [phyluxy@nus.edu.sg](mailto:phyluxy@nus.edu.sg), [wxguo@xmu.edu.cn](mailto:wxguo@xmu.edu.cn)

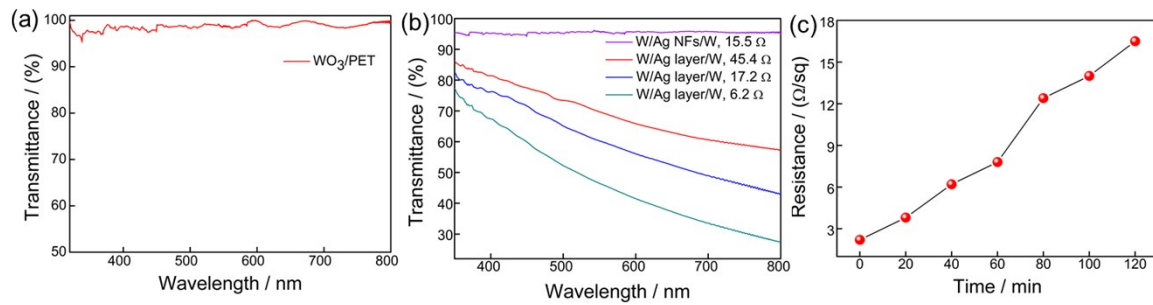


**Figure S1.** (a) Transmittance spectral of WO<sub>3</sub> sputtered on PET substrate for 2min. (b) Transmittance spectral of Ag sputtered on PET substrate for 20, 40, 60 s. (c) The resistance change of Ag NFs in the strong oxidizing electrolyte.

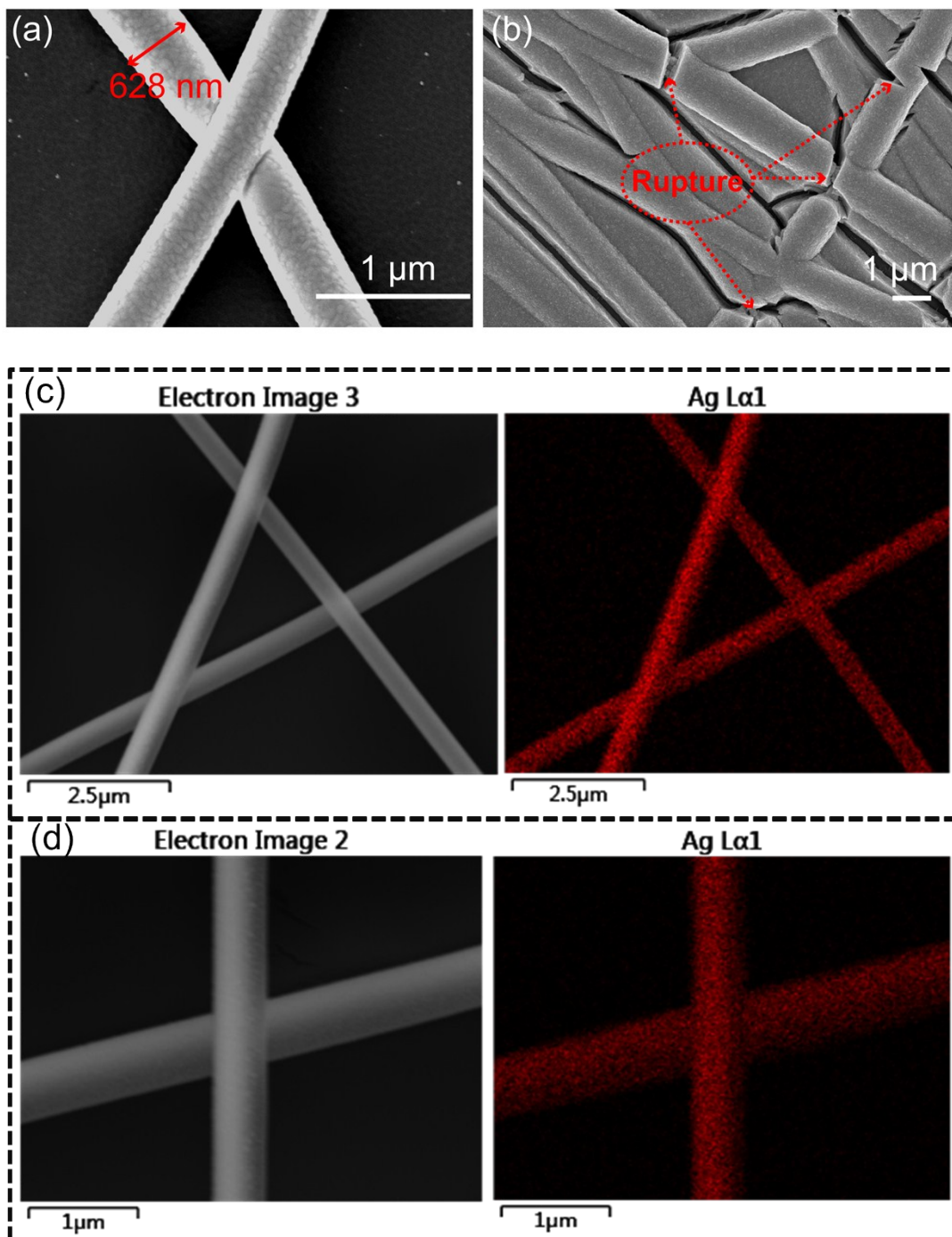


**Figure S2.** SEM of Ag NFs and  $\text{WO}_3$  film. (a) diameter of an Ag NF. (b)  $\text{WO}_3$  film for 2.5 h deposition time and the place where the red circle displays the break of the Ag NFs. (c) and (d) EDS mapping of Ag NFs mentioned in (a) with different magnification.

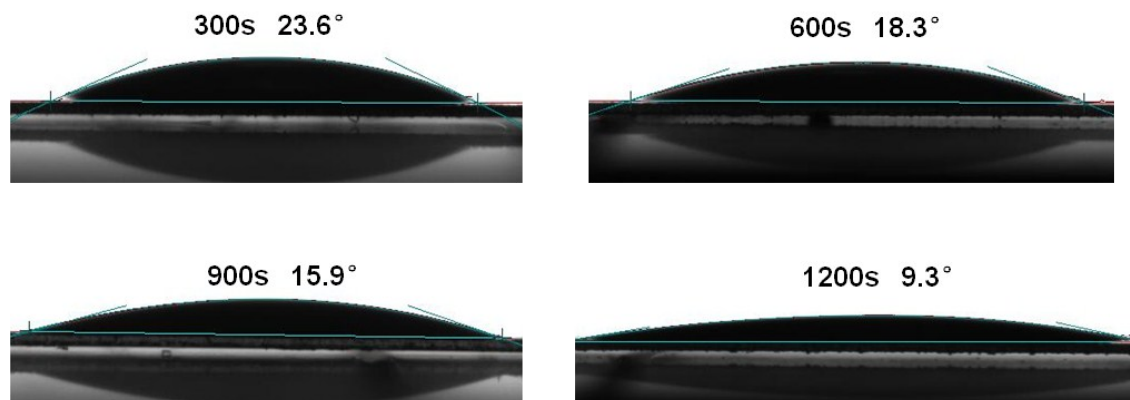


**Figure S3.** The variation tendency of surface hydrophilicity with the deposition of  $\text{WO}_3$  on flexible W/Ag NFs/W/PET.

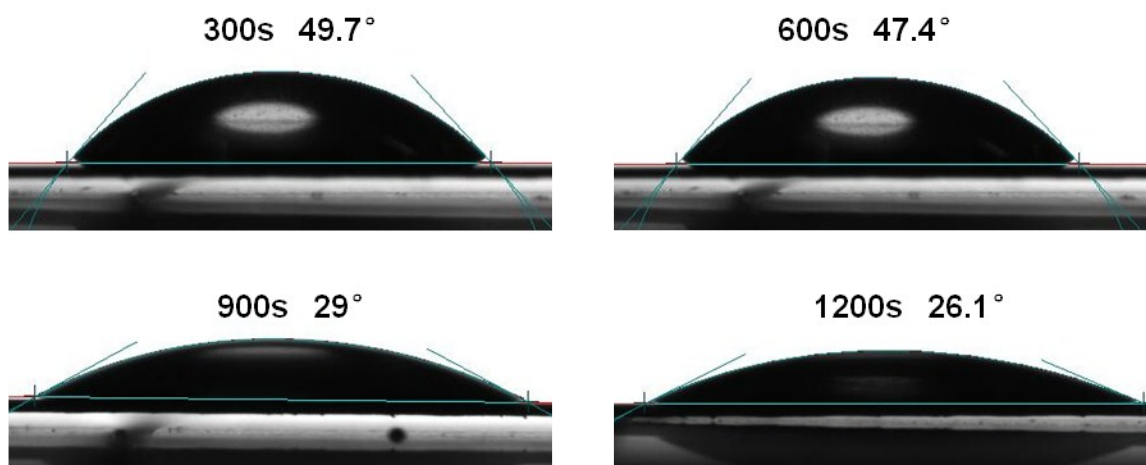


**Figure S4.** The variation tendency of surface hydrophilicity with the deposition of  $\text{WO}_3$  on ITO/PET.

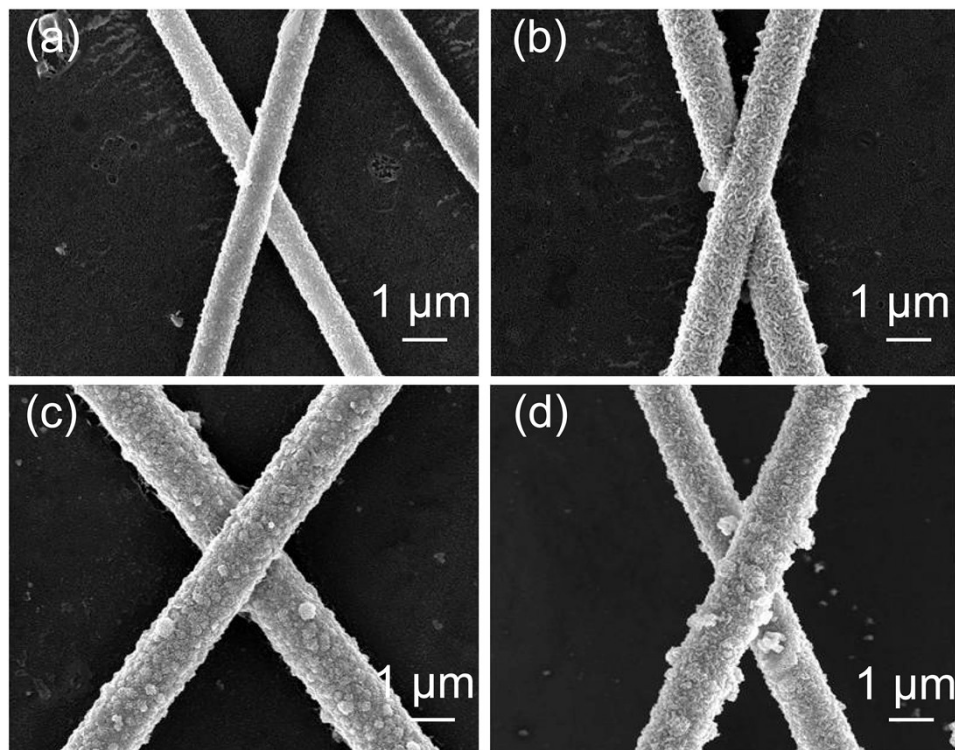


**Figure S5.** SEM images of  $\text{WO}_3$  deposited on the Ag NFs/PET films at different deposition time (a) 0 h, (b) 0.5 h, (c) 1 h, (d) 1.5 h. It is obvious that, in addition to depositing on the Ag NFs, there are hardly  $\text{H}_x\text{WO}_3$  nuclei on the gaps, which show that a bottom and a top  $\text{WO}_3$  thin layer play a decisive role during the electrodeposition.

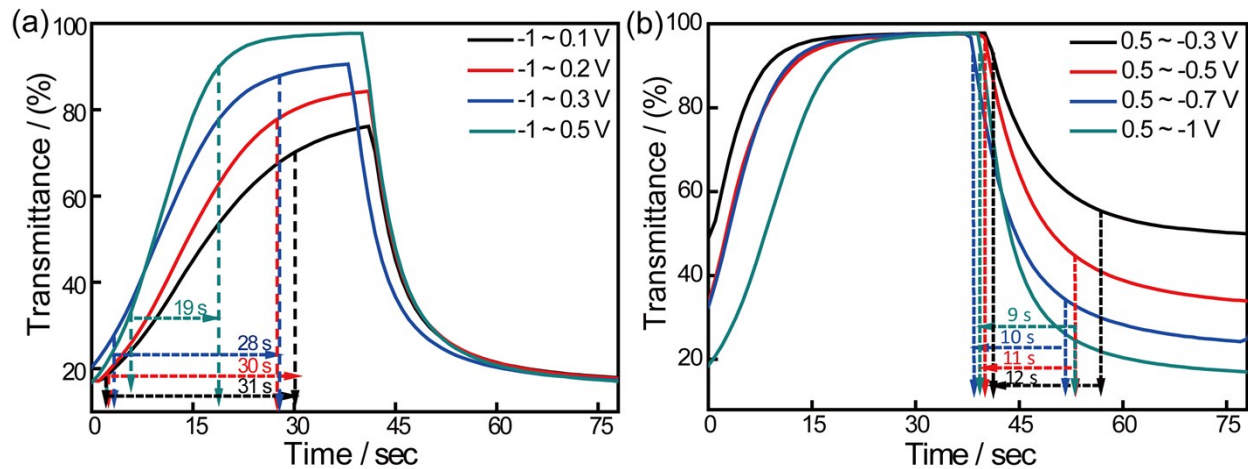
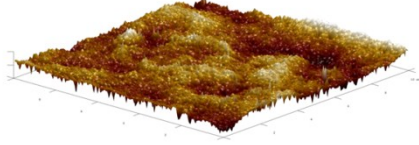


**Figure S6.** (a) and (b) Evolution of response characteristic of lamellar-porous structure  $\text{WO}_3$  films as a function of potentials.

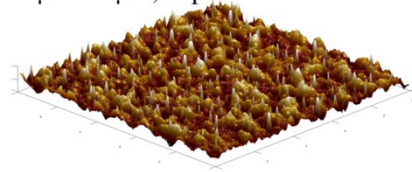
**Table 1.** The compare of electrochromic performance for WO<sub>3</sub>/ Ag-based ECDs.

Samples	method	$\Delta T$ (%)	CE (c <sup>-1</sup> cm <sup>2</sup> )	Coloration speed (s)	Bleaching speed (s)	Refs.
WO <sub>3</sub> - PEDOT:PSS/P EDOT:PSS/Ag grid/PET	Inkjet-printed	66	42	0.8	2.4	13
WO <sub>3</sub> /Ag grid/PET	Constant voltage electrochemical deposition	69	--	6.8	120	39
WO <sub>3</sub> /AgNW/N anopaper	Constant voltage electrochemical deposition	41	35	11.8	20.1	8
WO <sub>3</sub> /Ag/WO <sub>3</sub> / glass substrate	Magnetron sputtering	36	28	6.6	15.9	21
W <sub>18</sub> O <sub>49</sub> NW/Ag NW/PET	Drop coating	68	36	9	12.3	1
WO <sub>3</sub> / PEDOT:PSS/A g NWs/PET	Magnetron sputtering	50	--	0.18	0.25	29
WO <sub>3</sub> /Ag NN/PEDOT:PS S/PET	Magnetron sputtering	23	--	1.82	0.75	27
WO <sub>3</sub> /W/Ag NF/W/PET	Pulsed electrochemical deposition	90	59	9	19	This work

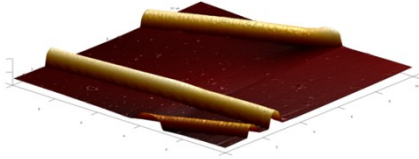
PET  
 $5\mu\text{m} \times 5\mu\text{m}$ ,  $R_q = 0.998\text{ nm}$



WO<sub>3</sub>/PET  
 $5\mu\text{m} \times 5\mu\text{m}$ ,  $R_q = 12\text{ nm}$



WO<sub>3</sub>/Ag NFs/WO<sub>3</sub>/PET  
 $5\mu\text{m} \times 5\mu\text{m}$ ,  $R_q = 62\text{ nm}$



ITO/PET  
 $5\mu\text{m} \times 5\mu\text{m}$ ,  $R_q = 2.55\text{-}3.06\text{ nm}$

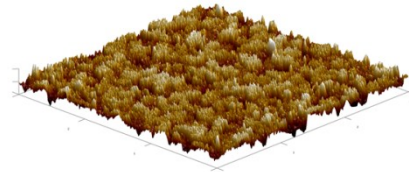


Figure S7. The AFM of PET, WO<sub>3</sub>/PET, WO<sub>3</sub>/Ag NFs/WO<sub>3</sub>/PET and ITO/PET.

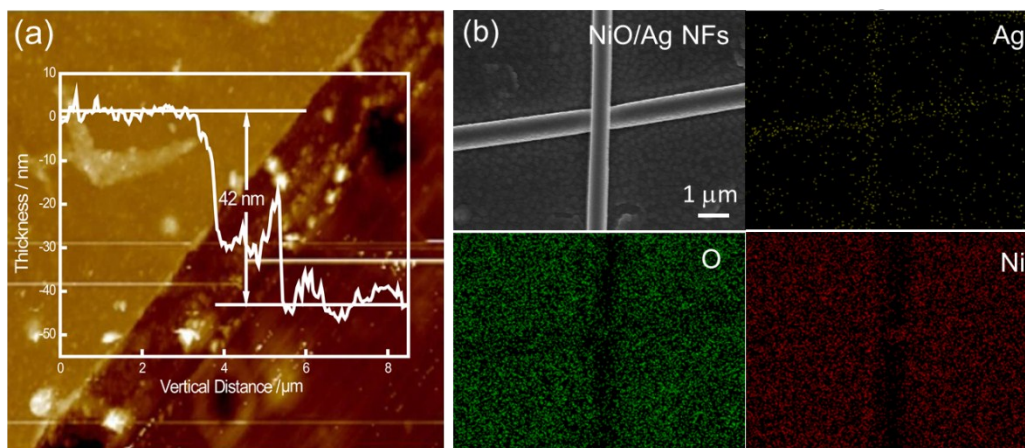


Figure S8. (a) AFM and (b) SEM and EDS mapping of NiO.